ANTIOXIDANTS & REDOX SIGNALING
Volume 10, Number 4, 2008

DOI: 10.1089/ars.2007.1521

Original Research Communication

Rac and PI3 Kinase Mediate Endothelial Cell–Reactive Oxygen Species Generation During Normoxic Lung Ischemia

QUNWEI ZHANG, SHAMPA CHATTERJEE, ZHIHUA WEI, WEI DONG LIU, and ARON B. FISHER

ABSTRACT

Abrupt reduction of flow (ischemia) leads to endothelial cell membrane depolarization, NADPH oxidase activation, and reactive oxygen species (ROS) generation in isolated rat and mouse lungs and in flow-adapted endothelial cells *in vitro*. Here we evaluated the role of PI-3-kinase and rac in activation of endothelial NADPH oxidase. Endothelium of isolated perfused mouse lungs labeled with 2′,7′-dichlorodihydrofluorescein (H_2DCF) or hydroethidine (HE) showed increased ROS generation with ischemia; these results were supported by TBARS measurement in whole-lung homogenate and by *in vitro* studies using flow-adapted mouse pulmonary microvascular endothelial cells. Ischemia-induced ROS generation in intact lung or isolated cells was blocked by pretreatment with *Clostridium difficile* toxin B, a rac inhibitor, and by wortmannin or LY294002, PI3 kinase inhibitors. In cells, immunofluorescence and immunoblot after subcellular fractionation showed ischemia-induced translocation of rac, $p47^{phox}$, and $p67^{phox}$ to the plasma membrane. Increased extracellular K^+ also resulted in rac translocation, providing evidence that this pathway is sensitive to alterations of endothelial cell membrane potential. These results indicate that PI-3-kinase and the small G protein rac are involved in the activation of endothelial cell NADPH oxidase that is associated with the acute loss of shear stress. *Antioxid. Redox Signal.* 10, 679–689.

INTRODUCTION

Endothelial cells normally are subjected to flow-induced shear stress associated with luminal blood flow. Based on *in vitro* studies, it is expected that endothelial cells *in situ* have adapted to these normal shear stresses (9). Previous studies in our laboratory with the isolated perfused rat and mouse lungs and *in vitro* cell-culture models indicated that endothelial cells *in situ* or flow-adapted cells *in vitro* respond to acute loss of flow (simulated ischemia) with a signaling cascade characterized by the generation of ROS (2, 4, 26, 28, 29, 32, 37, 40, 41). This response represents altered mechanotransduction as a result of the sudden decrease in endothelial cell shear stress. The initiating events appear to be endothelial cell membrane depolarization by inactivation of K_{ATP} channels, followed by the activation of endothelial membrane–localized NADPH oxidase (NOX) (4–6, 12, 13, 32, 34, 40). The NOX enzyme systems have been categorized into four groups depending on the membrane-bound flavoprotein component (8, 14, 19, 36). Our studies using lungs and endothelial cells from $gp91^{phox}$ gene-targeted mice indicate that NOX2 is the NADPH oxidase responsible for endothelial ROS generation in response to ischemia (4, 29, 40).

NOX2 has been best characterized in polymorphonuclear leukocytes. This enzyme complex is composed of two membrane-bound proteins ($p22^{phox}$ and $gp91^{phox}$) and at least four cytosolic proteins (rac, $p40^{phox}$, $p47^{phox}$, and $p67^{phox}$) (14, 19). On activation, the cytosolic proteins translocate to the membrane and associate with the membrane-bound subunits. Similar protein components and subcellular localization have been described for the NOX2 system in endothelial cells (21, 25). Activation of the NADPH oxidase is regulated by a complex set of reversible protein–protein interactions, yet the molecular details of these events are only poorly understood (22).

[1]Institute for Environmental Medicine, University of Pennsylvania Medical Center, Philadelphia, Pennsylvania.

Phosphorylation of the cytosolic proteins plays an important role in regulation of the interactions that ultimately lead to their recruitment to the plasma membrane (8, 30, 36). Stimulation of NADPH oxidase activity by guanine nucleotides provided evidence that a GTPase might play a role in activation of the enzyme complex (15, 30). Rac, a member of the Rho small-GTPase family, has been proposed as a regulator of the NADPH oxidase enzyme complex in both phagocytic and nonphagocytic cells (8, 30, 36). Phosphatidyl inositol-3 kinase (PI3K) also has been implicated in the activation of NADPH oxidase in various cell systems (1, 10, 20, 33, 39). In the present investigation, we propose that abrupt reduction of shear stress (ischemia) results in PI3K activation, which initiates translocation of rac and other cytosolic proteins from endothelial cytosol to plasma membrane, thereby resulting in activation of endothelial cell NADPH oxidase to generate ROS.

MATERIALS AND METHODS

Chemicals and reagents

DiI-acetylated low-density lipoprotein (DiI-AcLDL), hydroethidine (HE), and dichlorodihydrofluoroscein diacetate (H_2DCF) were obtained from Molecular Probes (Eugene, OR). Stock solutions of H_2DCF diacetate (5 m*M*) or HE (10 m*M*) were prepared in 100% ethanol and stored under N_2 at −20°C in the dark. Butylated hydroxytoluene, thiobarbituric acid, ferricytochrome *c* (cyt *c*) from horse heart, and bovine erythrocyte superoxide dismutase (SOD) were purchased from Sigma Chemical (St. Louis, MO). A kit for measurement of PI3K by ELISA was obtained from Echelon Biosciences (Salt Lake City, UT). Diphenyleneiodonium chloride (DPI), wortmannin, LY294002, and toxin B from *Clostridium difficile* were from Calbiochem (La Jolla, CA). Catalase was from Boehringer Mannheim (Indianapolis, IN). Antibodies to gp91^{phox}, p47^{phox}, p67^{phox}, and PI3K were purchased from Upstate Biotechnology (Lake Placid, NY). For secondary antibodies, Alexa Fluor 488 goat anti-rabbit IgG, rhodamine red goat anti-rabbit IgG, and goat anti-mouse IgG were purchased from Invitrogen (Carlsbad, CA); for use in the Odyssey system, IRDye 800 goat anti-mouse IgG and IRDye 700 goat anti-rabbit IgG were purchased from Rockland (Gilbertsvillle, PA). Anti-rac1 and rat anti-mouse CD31 were obtained from BD Biosciences (San Diego, CA). Protein assay reagent and γ-globulin were from Bio-Rad Laboratories (Hercules, CA). The rac-GFP plasmid was a gift of Dr. Martin Schwartz (University of Virginia). All chemicals used were of analytic grade.

Animals

Animal use was reviewed and approved by the University of Pennsylvania Institutional Animal Care and Use Committee. Male C57BL/6J mice weighing ~20 g were obtained from Jackson Labs (Bar Harbor, ME).

Isolated lung perfusion

The isolated perfused mouse-lung technique used for this study has been described previously (18, 32). In brief, mice were anesthetized with 50 mg/kg intraperitoneal sodium pentobarbital and continuously ventilated through a tracheal cannula with 5% CO_2 in air (BOC Group, Inc., Murray Hill, NJ). The chest was opened, and the pulmonary circulation was cleared of blood by gravity flow of perfusate through a cannula inserted in the main pulmonary artery, exiting from the transected left ventricle. The perfusate was Krebs' Ringer bicarbonate solution (KRB: NaCl, 118.45; KCl, 4.74; $MgSO_4 \cdot 7H_2O$, 1.17; KH_2PO_4, 1.18; and $NaHCO_3$, 24.87 in m*M*) plus 10 m*M* glucose and 5% dextran to maintain isotonicity. The heart–lung preparation was dissected *en bloc* and placed onto a 48 × 60 × 0.16-mm coverglass in a specially designed Plexiglas chamber with ports for tracheal and pulmonary artery cannulas. The cardiovascular ports were connected to a peristaltic pump that recirculated 30 ml perfusate at a constant flow rate of 2 ml/min through the vascular bed. The heart muscle was trimmed away, and a local anesthetic (0.05 mg xylazine) was injected subepicardially into the posterior wall of the right atrium to abolish lung-movement artifact due to contraction of the remaining cardiac muscle.

Intravital subpleural microvascular endothelial cell microscopy

Intravital microscopy was performed as previously described (4, 6, 27, 32, 34). In brief, the chamber was placed on the stage of an epifluorescence microscope fitted with a 60× objective (Nikon Diaphot TMD) and equipped with an optical filter changer (Lambda 10-2; Sutter Instrument Co. , Novato, CA), a Hamamatsu ORCA-100 digital camera (Hamamatsu Corp. , Bridgewater, NJ), and MetaMorph imaging software (Universal Imaging Corp. , Downingtown, PA). Excitation of the lung surface was accomplished with a mercury lamp fiberoptic light source and the appropriate filter set as follows: for DCF, 485 ± 5-nm excitation, HQ-41001b with 510 ± 10-nm emission; for HE, 480-nm excitation, 585 ± 25-nm emission.

For imaging studies, isolated lungs were shaded from direct light. Lungs were preperfused with H_2DCF (5 μ*M*) or HE (10 μ*M*) for 30 min to allow uptake of the fluorophore, and intravascular dye was then removed by 10-min perfusion with dye-free medium to reduce background fluorescence. In some experiments, wortmannin (100 n*M*) or toxin B (2.5 ng/ml) was added to the dye-loading solution during the preperfusion period. Wortmannin was used to inhibit phosphatidylinositol 3-kinase/mitogen-activated protein kinases (3) and toxin B as an inhibitor of small GTPases (31). Images were acquired at 1-min intervals during a 10- to 15-min control period of continuous perfusion. Then the perfusion pump was abruptly stopped ("ischemia"); ventilation was stopped only briefly (<15 sec) to permit collection of fluorescence images from randomly selected areas of each lung. For quantitation, an area of interest containing one or more endothelial cells was outlined, and the change of the fluorescence intensity compared with baseline was calculated. Values for five to seven areas of interest (endothelial cells) were averaged to obtain a mean value for each lung.

DCF and HE fluorescence and TBARS in lung homogenates

Lung oxidation of fluorophores was also determined by assay of whole-lung homogenate. Lungs were preperfused with

H_2DCF (5 μM) or HE (10 ÊM) for 30 min to allow uptake of the fluorophore, and intravascular dye was then removed by 10-min perfusion with dye-free medium to reduce background fluorescence. In some lungs, wortmannin or toxin B was added during the perfusion period. After 60 min of continuous perfusion or at the end of 60-min ischemia, lungs were rapidly frozen in liquid N_2 and homogenized under N_2 in 10 volumes of ice-cold PBS containing 0.2% butylated hydroxytoluene. The fluorescence of the homogenate was determined by using a spectrofluorometer (PTI, Bricktown, NJ) with 485-nm excitation and 510-nm emission for DCF (4, 37, 41) or 480-nm excitation and 585-nm emission for HE (2).

Lipid peroxidation in lung homogenates was evaluated by assay for thiobarbituric acid reactive substances (TBARS) as described previously (18, 41). Lungs were subjected to 60 min of continuous perfusion or ischemia. An aliquot of lung homogenate prepared as described earlier was extracted with trichloroacetic acid and reacted with thiobarbituric acid at 95°C for 15 min (18). TBARS were calculated by using an extinction coefficient of 1.56×10^5 M/cm at 535 nm (11).

Protein content of the lung homogenate was determined by the BioRad Coomassie blue binding assay with bovine γ-globulin as the standard.

Isolated mouse pulmonary endothelial cells (MPMVECs)

Pulmonary microvascular endothelial cells were isolated from mouse lungs as described previously (29, 40). In brief, mouse lungs were cleared of blood, minced finely, incubated with 0.1% collagenase at 37°C, and filtered through a sterile 100-μm cell strainer to remove macrophages. The cell suspension was incubated with platelet endothelial cell adhesion molecule (PECAM) antibody (rat anti-mouse CD31) added to the cell suspension, and endothelial cells were isolated by magnetic bead separation by using sheep anti-rat IgG–coated Dynabeads (Dynal Biotech, Oslo, Norway). The Dynabeads with attached cells were seeded onto gelatin-coated flasks and allowed to grow to 80% confluence before use. The endothelial phenotype of the preparation was confirmed by demonstrating cellular uptake of Dil-acetylated low-density lipoprotein (DiI-Ac-LDL) and reactivity to anti-CD-31 (29, 40).

Endothelial cell culture and flow adaptation

MPMVECs were adapted to laminar flow *in vitro* before study of the effects of altered shear stress. The shear stress chosen was 5–10 dyn/cm^2, which is in the generally accepted physiologic range and in our studies is sufficient to produce a flow-adapted state (12, 13, 26, 29, 37, 38). Cells were cultured in Dulbecco's modified Eagle medium (DMEM) supplemented with 10% fetal bovine serum, nonessential amino acids, and penicillin/streptomycin.

Three different systems were used for flow adaptation, depending on the intended use. In the first model, MPMVECs in complete medium (pH 7.4) were placed on a glass or plastic slide (44 × 20 mM) that had been coated with 0.2% gelatin and allowed to grow for at least 24 h until they became fully confluent. The glass slide then was placed in a flow chamber (Confocal Imaging chamber RC-30; Warner Instruments, Hamden, CT), and cells were cultured for 24 h at 37° under either static conditions or continuous laminar flow at 5 dyn/cm^2. The volume of recirculating perfusate was 10 ml, and the volume of the chamber is ~200 μl. The perfusate was complete culture medium supplemented with 25 mM HEPES, pH 7.4, and equilibrated with 5% CO_2 in air. These cells were used for immunofluorescence detection by confocal imaging.

As a second model, cells were cultured on plastic slides and were flow adapted at 10 dyn/cm^2 in a chamber that was constructed to fit in the cuvette holder of a spectro(fluoro)meter (26). Control cells were cultured under static conditions except for a 30-min period of flow just before measurement to load cyt *c*. These cells were used to measure superoxide production.

The third model for cell adaptation to flow was the use of an artificial capillary system (Cell Max; FiberCell Systems, Inc., Frederick, MD), as described previously (12, 29, 37, 38). The capillaries were precoated with 0.2% gelatin. Cells from five confluent T75-cm^2 flasks of MPMVECs were seeded per cartridge and cultured under laminar flow at 5 dyn/cm^2 for 48 h. Oxygenation of cells during ischemia is maintained by flow through abluminal ports. These cells were used for subcellular fractionation studies to determine protein translocation. Control cells were cultured under static conditions. It was not possible to study localization of NOX2 components during continuous flow because a period of stop flow (ischemia) was necessary to remove cells from the chamber.

Cellular localization of NADPH oxidase proteins

Membrane localization of NADPH oxidase proteins was studied by immunofluorescence for gp91^{phox}, p47^{phox}, and p67^{phox}. Rac localization was studied with a rac-GFP fusion protein. Rac-GFP plasmid DNA was cloned into pGFPC1 by using Btxl and Sal I sites and was amplified in *Escherichia coli* that contain an F plasmid Rac-GFP. Plasmid DNA was isolated by the Plasmid Midi kit (QIAGEN, Valencia, CA) and transfected into MPMVECs by Nucleofector Technology (Amaxa GmbH, Germany). MPMVECs were fixed with 4% paraformaldehyde, embedded in paraffin, and incubated with anti-gp91^{phox} , anti-p67^{phox}, or anti-p47^{phox} in phosphate-buffered saline (PBS) containing 3% bovine serum albumin (BSA) at 4°C overnight followed by the appropriate secondary antibody. Slides were sealed and observed with fluorescence microscopy. In some experiments, cells cultured under static conditions were exposed to medium containing either 12 or 24 mM KCl; these solutions were prepared by reducing NaCl an equivalent amount to maintain iso-osmolality. After 10 min of incubation plus or minus 2.5 ng/ml toxin B or 100 nM wortmannin, cells were fixed and evaluated for rac translocation.

For subcellular fractionation studies, cells were cultured under static conditions (control) or were flow adapted and subjected to ischemia in the artificial capillary system. Cells were harvested and removed from the cartridges with trypsin, sonicated, and subjected to differential sucrose-gradient centrifugation for isolation of plasma membrane and cytosol fractions (17). Membrane and cytosolic fractions were prepared, and protein from each fraction was subjected to SDS/PAGE; the electrophoresed proteins were transferred to a nitrocellulose membrane, blocked for 1 h with 5% milk in PBS, and incubated with anti-rac1, anti-p47^{phox}, and anti-p67^{phox} antibodies overnight. After washing, the membrane was incubated with either per-

oxidase-conjugated or IRDye-conjugated secondary antibody, as appropriate. The reaction was revealed with enhanced chemiluminescence (Amersham) or with the Odyssey imaging system (Li-Cor, Lincoln, NE) for quantitation.

Superoxide production

Superoxide anion radical ($O_2^{-\cdot}$) generation was evaluated by measurement of absorbance of cyt *c* (150 μM) in the presence of 20 U/ml SOD by using a Beckman DU640B (Beckman Instruments, Fullerton, CA) dual-beam spectrophotometer (3-nm slits). Inhibitors (wortmannin, LY294002, toxin B) when present were added during the final 30 min of flow before the onset of ischemia. For control experiments, cells grown under static conditions were subjected to flow for 30 min, which was then stopped during ROS detection. Spectra were recorded at 30-sec intervals during simulated ischemia in the real-time kinetic mode with resolution of 1 point each 15 sec (26). Reduction of cyt c by $O_2^{-\cdot}$ was measured by change in absorbance at 550 nm.

PI3K activity

To measure PI3K activity, MPMVECs under control conditions or treated with high (24 m*M*) K^+ with or without wortmannin (100 n*M*) were scraped from the culture dish and centrifuged. Anti-PI3K antibody was added to the supernatant (in concentrations as instructed in the assay kit from Echelon) and mixed in a slurry of protein A agarose beads to immunopre-

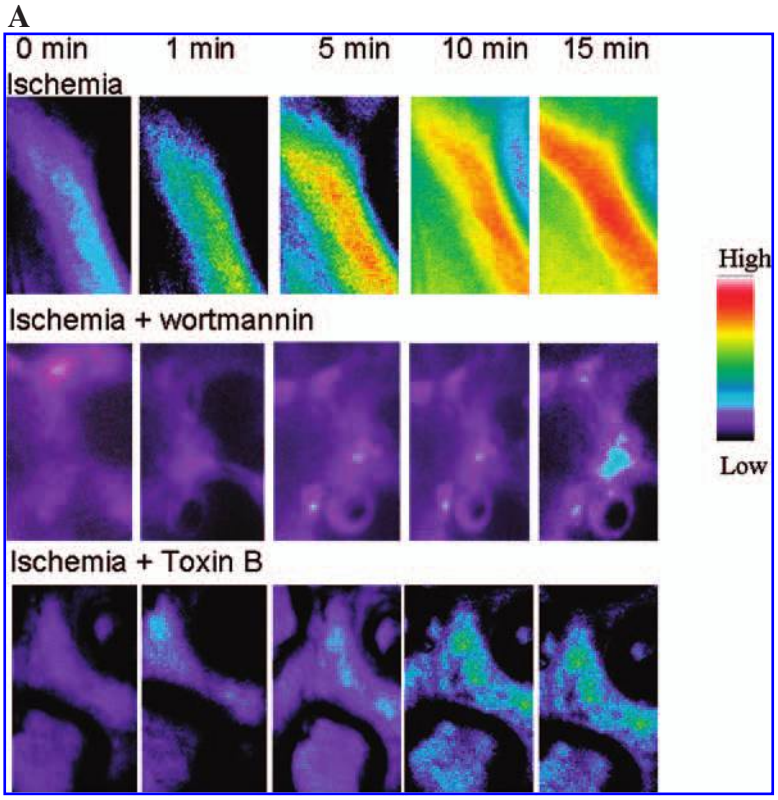

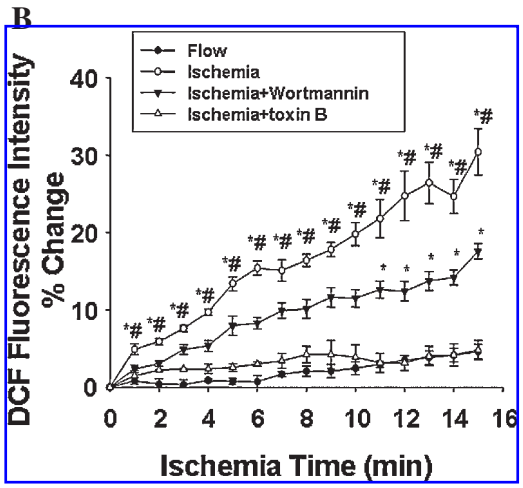

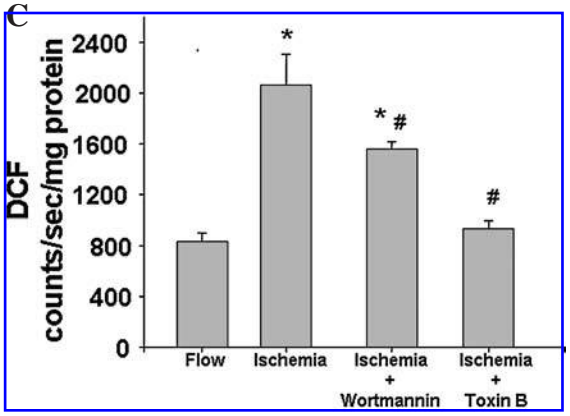

FIG. 1. Lung endothelial ROS production with ischemia as measured by dichlorofluorescein (DCF) fluorescence. (**A**) Imaging of subpleural endothelial cells in the intact mouse lung. Lungs were pre-perfused with H_2DCF diacetate plus or minus inhibitors (wortmannin, 100 n*M*, or toxin B, 2.5 ng/ml) for 30 min, followed by dye-free perfusate for 10 min. Images were acquired at 1-min intervals for 5 min before and 15 min after global cessation of flow (ischemia). The time below the images indicates time after cessation of flow. All images were acquired by using the same gain settings. Images are in pseudocolor, as indicated by the intensity scale. (**B**) Quantitation of time course of DCF fluorescence intensity change with lung ischemia. Mean ± SEM change in fluorescence intensity of three to four lungs (each representing the average value for three to six endothelial cells) is plotted *versus* time for continuously perfused (control) or ischemic mouse lung. $*p < 0.05$ *versus* the corresponding control lung; $\#p < 0.05$ compared with ischemia. (**C**) Measurement of DCF fluorescence in lung homogenates. Lungs were continuously perfused (control) or subjected to 1-h ischemia in the absence or presence of inhibitors, as shown in (**A**). Lungs were homogenized, and the fluorescence in the supernatant was measured with a spectrofluorometer. Data are expressed as mean ± SEM of three to four lungs under each condition. $*p < 0.05$ *versus* flow; $\#p < 0.05$ *versus* ischemia. (For interpretation of the references to color in this figure legend, the reader is referred to the web version of this article at www.liebertonline.com/ars).

cipitate the protein. The immunoprecipitate was collected by centrifugation, washed, and used for an ELISA assay. The kit uses the production of PI(3,4,5)P3 from PI(4,5)P2 to measure PI3K activity. The PIP2 substrate was added directly to the immunoprecipitated enzyme bound to beads and incubated for 1 h. The PIP3 detector protein solution was added, and a microtiter detection plate reader was used to measure the colorimetric signal. All solutions and buffers (except the anti-PI3K antibody) were supplied with the kit.

Statistical analysis

Results are expressed as mean ± SEM generally for three to four lungs for each condition. For time-dependent studies, significant parametric differences among groups were evaluated with two-way analysis of variance; if the F value was statistically significant, groups were then compared at each time by one-way analysis of variance followed by Dunnett's t test. Comparison among conditions was evaluated with one-way analysis of variance and Bonferroni's test for multiple comparisons by using Sigma Stat (Jandel Scientific, San Raphael, CA). Differences were considered significant at $p < 0.05$.

RESULTS

Endothelial ROS generation with lung ischemia

The fluorophores H_2DCF and HE were used for imaging of subpleural microvessels to detect endothelial ROS generation with ischemia in mouse lungs. Essentially no change in fluorescence was found during continuous perfusion (control, images not shown). Increased fluorescence with both reporters (DCF and HE) was observed in 1 min and increased progressively during the subsequent 15 min after cessation of flow (Figs. 1 and 2). The increase in DCF and HE fluorescence with

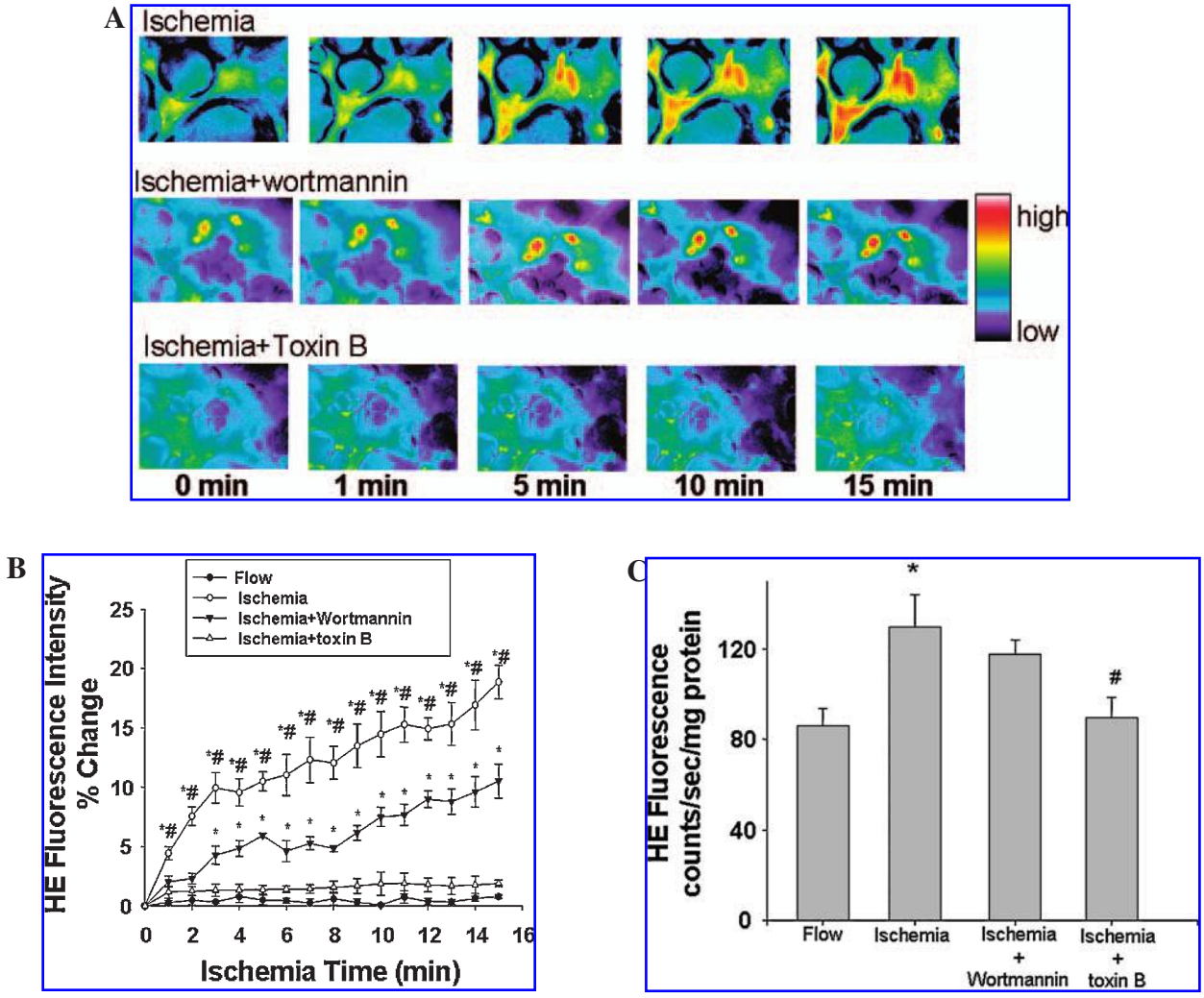

FIG. 2. Lung endothelial ROS production with ischemia as measured by hydroethidine (HE) fluorescence. (**A**) Imaging of subpleural endothelial cell in the intact mouse lung. (**B**) Quantitation of time course of HE fluorescence intensity change with lung ischemia. (**C**) Measurement of HE fluorescence in lung homogenates. The experimental protocols were the same as described in Fig. 1. (For interpretation of the references to color in this figure legend, the reader is referred to the web version of this article at www.liebertonline.com/ars).

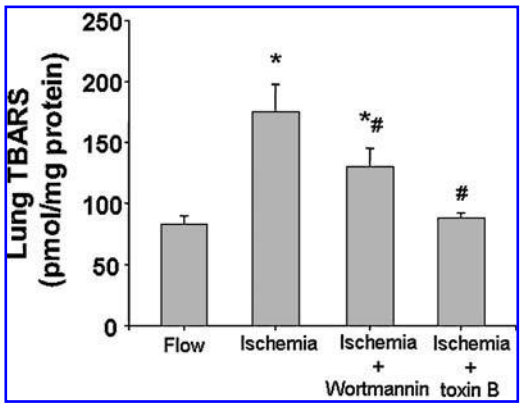

FIG. 3. Lipid peroxidation of isolated lungs during ischemia, as measured by thiobarbituric acid reactive substances (TBARS). The effects of ischemia in the absence or presence of wortmannin (100 n*M*) or toxin B (2.5 ng/ml) on lung content of TBARS was measured after 1 h of continuous perfusion (flow) or no flow (ischemia). Values are expressed as mean ± SEM of three to four lungs under each condition. $*p < 0.05$ *versus* flow; $\#p < 0.05$ *versus* with ischemia.

ischemia was abolished by pretreatment of lungs with toxin B and was markedly attenuated by pretreatment of lungs with wortmannin (see Figs. 1 and 2).

The results for imaging were confirmed by measuring fluorescence in lung homogenate after 60-min ischemia. DCF (Fig. 1C) and HE (Fig. 2C) fluorescence in lung homogenate after 60-min ischemia increased 2.5- and 1.5-fold, respectively, above that in control lungs (continuous perfusion). The increase in fluorescence was abolished by pretreatment with toxin B and partly inhibited by wortmannin.

TBARS in lung tissue were measured as an indicator of lipid peroxidation associated with ROS generation. TBARS measured after 60-min ischemia approximately doubled as compared with control (Fig. 3). The increase was completely blocked when the lungs were pretreated with toxin B and partially blocked by wortmannin.

ROS generation with flow cessation in flow-adapted endothelial cells in vitro

ROS generation in flow-adapted MPMVECs in response to abrupt cessation of flow was evaluated by continuous measurement of the reduction of cyt c added to the perfusate. This method measures extracellular generation of $O_2^{\cdot -}$ because cyt *c* remains in the extracellular space, and $O_2^{\cdot -}$ crosses the cellular plasma membrane relatively slowly. MPMVECs that were adapted to 10 dynes/cm^2 of shear stress for 24 h showed cyt c reduction within 10 sec and a progressive increase during the subsequent 5 min after flow cessation (Fig. 4). Pretreatment with wortmannin, LY294002, or toxin B significantly inhibited ROS generation by flow-adapted MPMVECs. Cells that had not been adapted to flow (static culture with 30-min perfusion) showed essentially no change in cyt *c* absorbance with flow cessation, and the inhibitors were without effect.

Translocation of NADPH oxidase components from cytosol to plasma membrane

Translocation of cytosolic proteins to the plasma membrane associated with flow cessation was studied by fluorescence imaging to show colocalization with gp91^{phox}, an integral membrane protein. Specificity of the antibody used for these studies was shown by the loss of immunoreactivity in gp91^{phox}-null endothelial cells (29). This result was confirmed in the present study (images not shown). MPMVECs transfected with rac-GFP were flow adapted (5 dynes/cm^2 for 24 h) and then subjected to 30 min of no flow (ischemia). Fluorescence imaging for GFP and immunostaining for gp91^{phox} indicated colocalization of the two proteins in the ischemic flow-adapted cells but not in the static cells (Fig. 5A). Staining was abolished by omission of the primary antibody (Fig. 5A). Because gp91^{phox} is a plasma membrane protein, the results indicate translocation of rac-GFP to the plasma membrane with ischemia. Translocation of rac-GFP with ischemia was blocked by pretreatment of cells with wortmannin or toxin B (Fig. 5A).

Co-localization experiments also were carried out with wild-type (nontransfected) MPMVECs to study translocation of p67^{phox} and p47^{phox}. Immunostaining of flow-adapted cells with

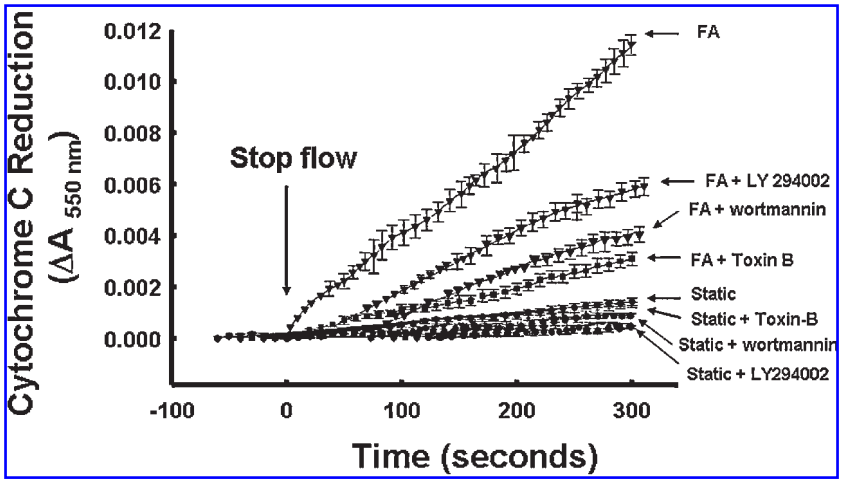

FIG. 4. $O_2^{\cdot -}$ generation with flow cessation in mouse pulmonary microvascular endothelial cells (MPMVECs). MPMVECs were flow adapted to 10 dynes/cm^2 for 24 h or cultured under static conditions in a flow chamber. Static cells were subjected to flow for 30 min. Inhibitors were added during the final 30 min of flow. Reduction of ferricytochrome c was measured for 1 min before and 5 min after stop of flow in the presence or absence of 100 n*M* wortmannin, 20 μM LY294002, or 2.5 ng/ml toxin B. Values are expressed as mean ± SEM for $n = 4$ experiments. FA, flow adapted.

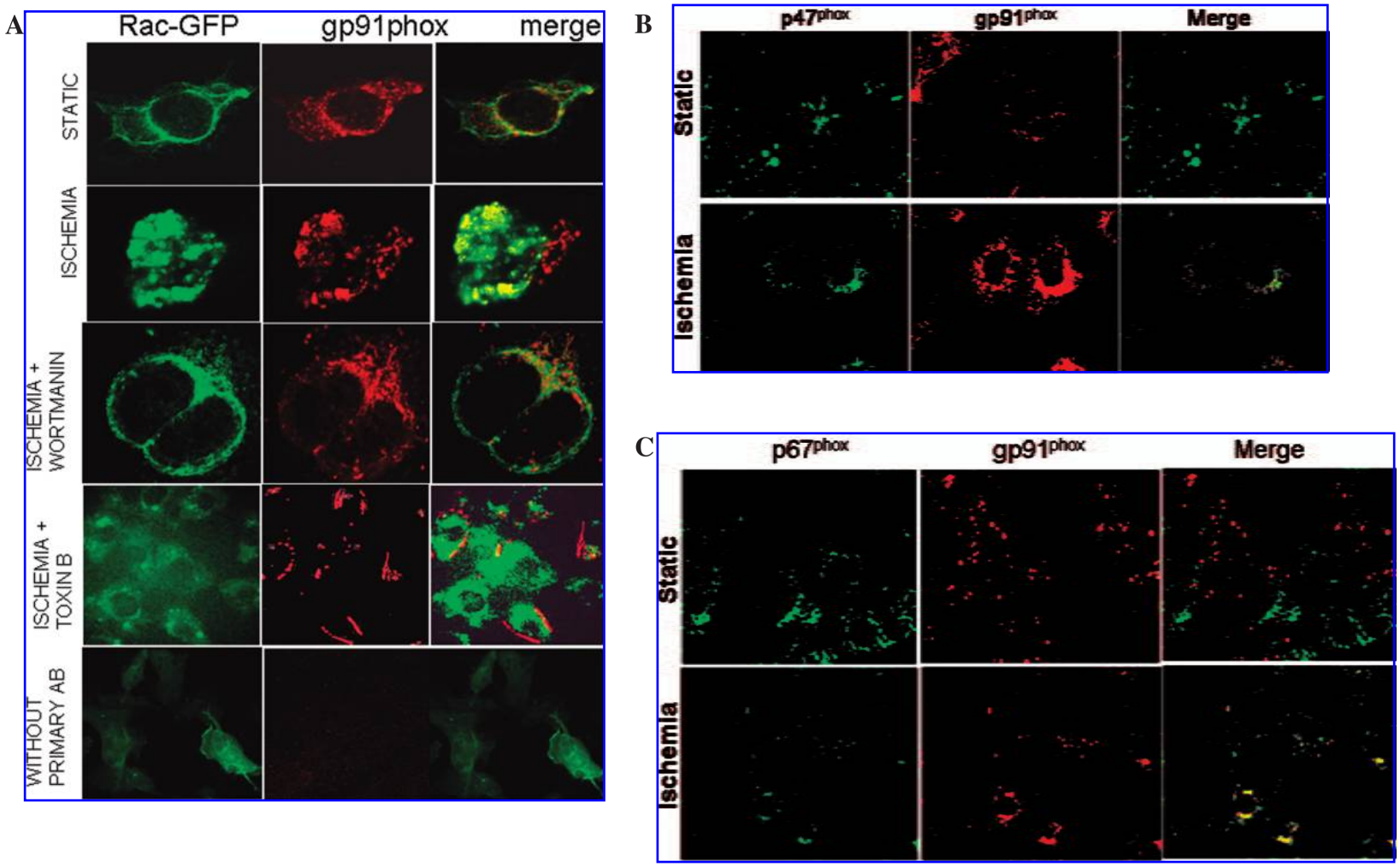

FIG. 5. Fluorescence microscopy for colocalization of rac 1, p67^{phox}, and p47^{phox} with gp91^{phox} during ischemia in MPMEVCs. MPMVECs were flow adapted to 5 dynes/cm^2 for 24 h in a confocal imaging chamber and then subjected to 30-min ischemia. MPMVECs cultured under static conditions were used as a control. (**A**) Rac-GFP–expressing cells were incubated with anti-gp91^{phox} (first antibody) and rhodamine red goat anti-rabbit IgG (second antibody). For ischemia plus toxin B, cells were pretreated with 10 μg/ml of toxin B and then subjected to ischemia. The panel labeled "without primary Ab" shows the lack of reaction when anti-gp91^{phox} was omitted. (**B, C**) Cells were incubated with anti-p47^{phox} (**B**) or anti-p67^{phox} (**C**) and anti-gp91^{phox} antibodies followed by Alexa Fluor 488 goat anti-rabbit (green) and rhodamine red goat anti-rabbit (red) antibodies. Yellow in the merge frame indicates colocalization of the gp91^{phox} with the other protein.

anti-p67^{phox} and anti-p47^{phox} antibodies indicated colocalization of fluorescence with anti-gp91^{phox} (Fig. 5B and C). For MPMVECs cultured under static conditions, no apparent colocalization for these proteins was noted. This result suggests that ischemia leads to translocation of both p67^{phox} and p47^{phox} from cytosol to the plasma membrane, where they associate with gp91^{phox}.

Translocation of cytosolic components to plasma membrane with ischemia also was studied with immunoblots of subcellular fractions from MPMVECs that were flow adapted in the artificial capillary system. This system was used to obtain a sufficiently large number of cells for isolation of subcellular fractions. Plasma membrane and cytosolic fractions were analyzed by Western blot with anti-rac 1, anti-p67^{phox}, and anti-p47^{phox} antibodies. In MPMVECs cultured under static conditions, these proteins showed greater reaction in the cytosolic fraction (Fig. 6). In flow-adapted endothelial cells subjected to simulated ischemia, a shift to greater expression in the membrane and decreased expression in the cytosolic fraction occurred (Fig. 6 and Table 1). This result is compatible with translocation of the proteins from cytosol to plasma membrane.

Our previous studies suggested that the translocation of cytosolic components of NADPH oxidase with ischemia could be secondary to endothelial cell membrane depolarization. To test this possibility, MPMVECs were incubated with [K^+] greater than the normal 6 m*M* to depolarize the plasma membrane. Incubation with 12 and 24 m*M* K^+ in statically cultured cells resulted in increased rac colocalization with membrane localized gp91^{phox} (Fig. 7A). Thus, these results indicate that membrane depolarization is sufficient to stimulate rac translocation. Depolarization (with 24 m*M* K^+) also resulted in a 67% increase in the activity of PI3K protein that could be immunoprecipitated from MPMVECs as compared with control cells (Fig. 7B). This increase in cellular PI3K activity was inhibited by pretreatment of MPMVECs with wortmannin (100 n*M*). Translocation of rac associated with membrane depolarization by 24 m*M* K^+ was blocked by toxin B (Fig. 7A) and also by wortmannin (Fig. 7B). Thus, rac translocation with endothelial cell membrane depolarization appears to require the activation of PI3K.

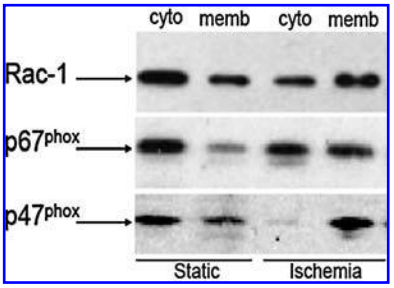

FIG. 6. Translocation of rac 1, p47^{phox}, and p67^{phox} proteins from cytosol to plasma membrane is stimulated by ischemia in flow-adapted MPMEVCs. MPMVECs were flow adapted to 5 dynes/cm^2 for 24 h in the artificial capillary and subjected to 30 min of ischemia. MPMVECs cultured under static conditions formed the control. The cytosolic (cyto) and membrane (memb) fractions were isolated and analyzed with Western blot (10 μg protein/lane) followed by detection by using chemiluminescence. Ischemia resulted in relative enrichment of the membrane fraction as compared with the static cells.

TABLE 1. TRANSLOCATION OF RAC-1, P67^{phox} AND P47^{phox}, FROM THE CYTOSOL TO THE PLASMA MEMBRANE AS DETERMINED BY SUBCELLULAR FRACTIONATION

	Memb/cyto	
	Static	*Ischemia*
rac-1	0.44 ± 0.08	2.5 ± 0.29
p67^{phox}	0.29 ± 0.05	2.3 ± 0.30
p47^{phox}	0.40 ± 0.05	2.1 ± 0.60

Cytosolic (cyto) and membrane (memb) fractions were analyzed with Western blot and quantified by using the Odyssey Imaging System. Protein loading was 20 mg/lane for cyto and 25 mg/lane for memb. The individual results for cyto and memb fractions represent arbitrary fluorescence units.

DISCUSSION

Our laboratory previously established an isolated perfused rat lung model that allowed the separation of the effects of ischemia from those of anoxia (18, 41). Imaging studies showed that abrupt cessation of flow led to a rapid (within 1 min) increase in ROS production by the pulmonary endothelium (32). Subsequent studies showed similar results with isolated mouse lungs (40). Results obtained with flow-adapted pulmonary endothelial cells indicated that the species of ROS was predominantly superoxide anions generated on the extracellular side of the plasma membrane (26). This observation and its inhibition by treatment with diphenyleneiodonium (29, 37, 40) are compatible with plasma-membrane NADPH oxidase as the ROS generator. The absence of ROS generation with ischemia in lungs (4) and flow-adapted pulmonary endothelial cells (29) from gp91^{phox} gene–targeted mice confirmed the role of the plasma membrane enzyme complex and indicates that NOX2 is the responsible NADPH oxidase isoform.

Measurements of fluorescence by imaging in the intact lung and assay of whole-lung homogenate were used in the present study to confirm ROS generation as a response to ischemia. The fluorescence probes used were HE and H_2DCF. Increased HE fluorescence with ischemia is compatible with NOX2-mediated generation of $O_2^{-}\cdot$. We have shown recently that extracellular $O_2^{\cdot -}$ can penetrate the plasma membrane of endothelial cells through Cl^- channels and react intracellularly with HE (23). Increased DCF fluorescence in endothelial cells of intact lungs and in lung homogenates after ischemia is compatible with the increased generation of H_2O_2 derived from dismutation of $O_2^{-}\cdot$. A secondary reaction is the superoxide-mediated activation of mitochondrial superoxide production (23). The conclusions reached based on analysis of fluorophores were supported by demonstrating increased TBARS with ischemia in whole mouse lung homogenate. TBARS measurement has been used as an index of lipid peroxidation, although it is known to be nonspecific, because various interfering or reactive substances are

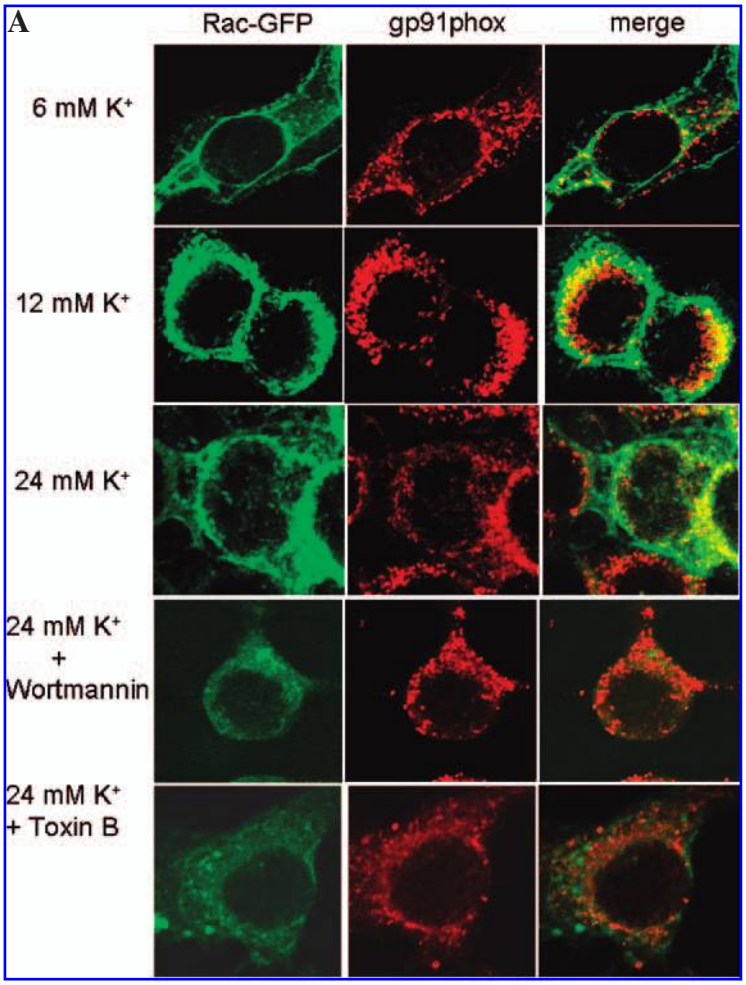

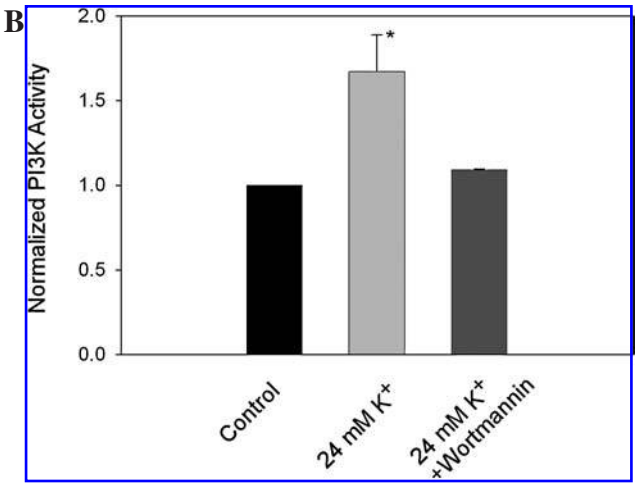

FIG. 7. Depolarization of MPMVEC membrane with high K^+. (**A**) Translocation of rac 1 to the plasma membrane. MPMVECs grown on coverslips were transfected with RacGFP. Cells were treated with 6, 12, or 24 m*M* K^+ for 5–10 min. Cells were fixed, permeabilized, and incubated with anti-$gp91^{phox}$ (primary antibody) and rhodamine red goat anti-rabbit IgG (secondary antibody). Fluorescence images were captured to show Rac-GFP (green) and $gp91^{phox}$ (red) localization. Yellow in the merge frame indicates colocalization of the two proteins. (**B**) PI3K activity. PI3Kinase activity in MPMVECs was measured with an ELISA method that detects the production of PIP3 from PIP2 by the PI3K present in the cell lysate. Cells were control (6 m*M* K^+), incubated in high K^+ (24 m*M*) , or incubated in high K^+ in the presence of 100 n*M* wortmannin, as in (**A**). The results were normalized to the PI3K activity in control cells. $*p < 0.05$ *versus* control. (For interpretation of the references to color in this figure legend, the reader is referred to the web version of this article at www.liebertonline.com/ars).

present. Our previous studies with the rat lung ischemia model have shown that TBARS in lung tissue increase significantly and reproducibly during 30–60 min of ischemia and support the fluorescence measurements of ROS (2, 4, 7, 18, 41, 42). Further, our studies have demonstrated excellent correlation between TBARS and measurements of conjugated dienes (16, 18, 41) or diphenylpyrenylphosphine (DPPP) fluorescence (27, 40). This latter is a fluorophore that reacts specifically with lipid hydroperoxides (27).

Our previous results demonstrated inhibition of ischemia-mediated ROS production by pretreatment of perfused lungs with PR39, providing evidence that assembly of the NADPH oxidase is required for ROS generation (4). PR39 is a peptide inhibitor of SH3 domains that blocks assembly of the oxidase.

The present study investigated the role of rac in the assembly of endothelial NADPH oxidase in response to altered shear stress. Rac has been shown in neutrophils and other cell types to be an important regulator of protein translocation and NADPH oxidase activation (24). The present study shows translocation of rac-1, as well as $p47^{phox}$ and $p67^{phox}$, to the plasma membrane of MPMVECs that were subjected to ischemia. ROS generation was inhibited by pretreatment with toxin B, as indicated by fluorescence and TBARS measurements in the intact lung and by measurement of $O_2^{-\cdot}$ production in flow-adapted endothelial cells. Toxin B is an inhibitor of small GTP-binding proteins including rac. Thus, translocation of rac appears to be necessary for activation of NOX2 in pulmonary microvascular endothelium in response to the altered shear stress associated with ischemia.

Our previous studies with the isolated rat lung indicated that ischemia results in release of NO that is blocked by the presence of wortmannin (3). In the present study, ROS generation with ischemia was suppressed when lungs were pretreated with wortmannin. ROS generation by flow-adapted cells subjected to ischemia also was inhibited by wortmannin or by LY204002, two chemically distinct inhibitors of PI3K. By an ELISA assay, treatment of MPMVECs with wortmannin did block the activation of PI3K. Thus, these results suggest activation of PI3K with ischemia, with the caveat that wortmannin also inhibits other related kinases (35). Evidence exists from other cell systems that activation of NADPH oxidase requires PI3K activity (1, 10, 20, 33, 39). Further, the presence of wortmannin in the present study inhibited the translocation of rac-GFP to the plasma membrane. Thus, the present results suggest that PI3 kinase activation is required for rac-1 translocation, NADPH oxidase activation, and subsequently increased ROS generation in the response of flow-adapted endothelial cells to loss of shear stress.

The mechanism for activation of rac by ischemia is not fully understood. Our previous studies showed that acute loss of shear stress (ischemia) results in endothelial cell membrane depolarization mediated by inactivation of the K_{ATP} channel (4–6, 12, 13, 32, 34, 40). Studies with perfused lung and isolated cell models of ischemia showed that both endothelial cell membrane depolarization and ROS generation were blocked by the presence of cromakalim (or its L isomer, lemakalim), a K_{ATP} channel agonist (6, 29, 32, 40). The responses of the plasma-membrane potential and ROS generation to ischemia were markedly diminished in endothelial cells that did not express K_{ATP} channels (13, 29, 40). To demonstrate that membrane potential is "upstream" of ROS, "knockout" of the NADPH oxidase ($gp91^{phox}$) abolished ROS production with ischemia but had no effect on the change in cell-membrane potential (40). By fluorescence imaging techniques, depolarization of the endothelial cell preceded the increased generation of ROS (26, 32). Thus, cell-membrane depolarization occurring with the onset of ischemia appears to be the stimulus for the subsequent activation of NADPH oxidase. The use of high extracellular K^+ to depolarize the endothelial cell membrane was shown in a previous study to activate ROS production by NADPH oxidase (NOX2) in endothelial cells of the perfused rat and mouse lung (4). High K^+ in the present study resulted in activation of PI3K and rac translocation. A study from another laboratory indicated that plasma membrane depolarization also results in the translocation of rac to the cell membrane and ROS generation in endothelial cells from the human umbilical vein (31). Thus, we postulate a linkage between cell-membrane K_{ATP} channels, cell-membrane potential, PI3K activation, rac translocation, and ROS production, although the molecular basis for initiation of the cascade remains to be determined.

ACKNOWLEDGMENTS

This work was supported by National Heart, Lung, and Blood Institute grants HL-60290 and HL-75587 and grant support to Dr. Qunwei Zhang from the American Lung Association (RG-872-N). The present address of Dr. Zhang is the Department of Environmental and Occupational Health Sciences, University of Louisville, Louisville, KY. We thank Kris DeBolt for assistance with cell culture, Dr. Yefim Manevich for advice regarding measurement of superoxide production, Dr. Martin Schwartz for the rac-GFP plasmid, and Jennifer Rossi and Susan Turbitt for typing the manuscript. This study was presented in part at the Experimental Biology meeting in San Diego, CA, in April 2005.

ABBREVIATIONS

BSA, bovine serum albumin; cyt *c*, ferricytochrome *c*; DCF, dichlorofluorescein; DiI-AcLDL, diI-acetylated low-density lipoprotein; DPI, diphenyleneiodonium (DPI); H_2DCF, 2′,7′-dichlorodihydrofluorescein; HE, hydroethidine; I/R, ischemia/reperfusion; KRB, Krebs' Ringer bicarbonate solution; MPMVECs, mouse pulmonary microvascular endothelial cells; NOX, NADPH oxidase; NF-κB, nuclear factor κB; PBS, phosphate-buffered saline; phosphatidylinositol-3 kinase (PI3K); ROS, reactive oxygen species; SOD, superoxide dismutase; TBARS, thiobarbituric acid reactive substances; Toxin B, *Clostridium difficile* toxin B.

REFERENCES

1. Ago T, Kuribayashi F, Hiroaki H, Takeya R, Ito T, Kohda D, and Sumimoto H. Phosphorylation of p47phox directs phox homology domain from SH3 domain toward phosphoinositides, leading to phagocyte NADPH oxidase activation. *Proc Natl Acad Sci U S A* 100: 4474–4479, 2003.
2. Al-Mehdi AB, Shuman H, and Fisher AB. Intracellular generation of reactive oxygen species during nonhypoxic lung ischemia. *Am J Physiol* 272: L294–L300, 1997.
3. Al-Mehdi AB, Song C, Tozawa K, and Fisher AB. Ca2+- and phosphatidylinositol 3-kinase-dependent nitric oxide generation in lung endothelial cells in situ with ischemia. *J Biol Chem* 275: 39807–39810, 2000.
4. Al-Mehdi AB, Zhao G, Dodia C, Tozawa K, Costa K, Muzykantov V, Ross C, Blecha F, Dinauer M, and Fisher AB. Endothelial NADPH oxidase as the source of oxidants in lungs exposed to ischemia or high K^+. *Circ Res* 83: 730–737, 1998.
5. Al-Mehdi AB, Zhao G, and Fisher AB. ATP-independent membrane depolarization with ischemia in the oxygen-ventilated isolated rat lung. *Am J Respir Cell Mol Biol* 18: 653–661, 1998.
6. Al-Mehdi AB, Zhao G, Tozawa K, and Fisher AB. Depolarization-associated iron release with abrupt reduction in pulmonary endothelial shear stress in situ. *Antioxid Redox Signal* 2: 335–345, 2000.

7. Ayene IS, Dodia C, and Fisher AB. Role of oxygen in oxidation of lipid and protein during ischemia/reperfusion in isolated perfused rat lung. *Arch Biochem Biophys* 296: 183–189, 1992.
8. Bokoch GM and Knaus UG. NADPH oxidases: not just for leukocytes anymore! *Trends Biochem Sci* 28: 502–508, 2003.
9. Braddock M, Schwachtgen JL, Houston P, Dickson MC, Lee MJ, and Campbell CJ. Fluid shear stress modulation of gene expression in endothelial cells. *News Physiol Sci* 13: 241–246, 1998.
10. Brown GE, Stewart MQ, Liu H, Ha VL, and Yaffe MB. A novel assay system implicates PtdIns(3,4)P(2), PtdIns(3)P, and PKC delta in intracellular production of reactive oxygen species by the NADPH oxidase. *Mol Cell* 11: 35–47, 2003.
11. Buege JA and Aust SD. Microsomal lipid peroxidation. *Methods Enzymol* 52: 302–310, 1978.
12. Chatterjee S, Al-Mehdi AB, Levitan I, Stevens T, and Fisher AB. Shear stress increases expression of a KATP channel in rat and bovine pulmonary vascular endothelial cells. *Am J Physiol Cell Physiol* 285: C959–C967, 2003.
13. Chatterjee S, Levitan I, Wei Z, and Fisher AB. KATP channels are an important component of the shear-sensing mechanism in the pulmonary microvasculature. *Microcirculation* 13: 633–644, 2006.
14. Cross AR and Segal AW. The NADPH oxidase of professional phagocytes: prototype of the NOX electron transport chain systems. *Biochim Biophys Acta* 1657: 1–22, 2004.
15. Doussiere J, Pilloud MC, and Vignais PV. Activation of bovine neutrophil oxidase in a cell free system: GTP-dependent formation of a complex between a cytosolic factor and a membrane protein. *Biochem Biophys Res Commun* 152: 993–1001, 1988.
16. Eckenhoff RG, Dodia C, Tan Z, and Fisher AB. Oxygen-dependent reperfusion injury in the isolated rat lung. *J Appl Physiol* 72: 1454–1460, 1992.
17. Fisher AB and Dodia C. Role of phospholipase A2 enzymes in degradation of dipalmitoylphosphatidylcholine by granular pneumocytes. *J Lipid Res* 37: 1057–1064, 1996.
18. Fisher AB, Dodia C, Tan ZT, Ayene I, and Eckenhoff RG. Oxygen-dependent lipid peroxidation during lung ischemia. *J Clin Invest* 88: 674–679, 1991.
19. Fisher AB, and Zhang G. NADPH and NADPH Oxidase. In: *Encyclopedia of Respiratory Medicine*, edited by Laurent GJ and Shapiro SD. New York: Elsevier, 2006, pp. 77–83.
20. Frey RS, Gao X, Javaid K, Siddiqui SS, Rahman A, and Malik AB. Phosphatidylinositol 3-kinase gamma signaling through protein kinase Czeta induces NADPH oxidase-mediated oxidant generation and NF-kappaB activation in endothelial cells. *J Biol Chem* 281: 16128–16138, 2006.
21. Griendling KK, Sorescu D, and Ushio-Fukai M. NAD(P)H oxidase: role in cardiovascular biology and disease. *Circ Res* 86: 494–501, 2000.
22. Groemping Y, Lapouge K, Smerdon SJ, and Rittinger K. Molecular basis of phosphorylation-induced activation of the NADPH oxidase. *Cell* 113: 343–355, 2003.
23. Hawkins BJ, Madesh M, Kirkpatrick CJ, and Fisher AB. Superoxide flux in endothelial cells via the chloride channel-3 mediates intracellular signaling. *Mol Biol Cell* 18: 2002–2012, 2007.
24. Hordijk PL. Regulation of NADPH oxidases: the role of Rac proteins. *Circ Res* 98: 453–462, 2006.
25. Li JM and Shah AM. Intracellular localization and preassembly of the NADPH oxidase complex in cultured endothelial cells. *J Biol Chem* 277: 19952–19960, 2002.
26. Manevich Y, Al-Mehdi A, Muzykantov V, and Fisher AB. Oxidative burst and NO generation as initial response to ischemia in flow-adapted endothelial cells. *Am J Physiol Heart Circ Physiol* 280: H2126–H2135, 2001.
27. Matot I, Manevich Y, Al-Mehdi AB, Song C, and Fisher AB. Fluorescence imaging of lipid peroxidation in isolated rat lungs during nonhypoxic lung ischemia. *Free Radic Biol Med* 34: 785–790, 2003.
28. Matsuzaki I, Chatterjee S, Debolt K, Manevich Y, Zhang Q, and Fisher AB. Membrane depolarization and NADPH oxidase activation in aortic endothelium during ischemia reflect altered mechanotransduction. *Am J Physiol Heart Circ Physiol* 288: H336–H343, 2005.
29. Milovanova T, Chatterjee S, Manevich Y, Kotelnikova I, Debolt K, Madesh M, Moore JS, and Fisher AB. Lung endothelial cell proliferation with decreased shear stress is mediated by reactive oxygen species. *Am J Physiol Cell Physiol* 290: C66–C76, 2006.
30. Seifert R, Burde R, and Schultz G. Activation of NADPH oxidase by purine and pyrimidine nucleotides involves G proteins and is potentiated by chemotactic peptides. *Biochem J* 259: 813–819, 1989.
31. Sohn HY, Keller M, Gloe T, Morawietz H, Rueckschloss U, and Pohl U. The small G-protein Rac mediates depolarization-induced superoxide formation in human endothelial cells. *J Biol Chem* 275: 18745–18750, 2000.
32. Song C, Al-Mehdi AB, and Fisher AB. An immediate endothelial cell signaling response to lung ischemia. *Am J Physiol Lung Cell Mol Physiol* 281: L993–L1000, Corrigenda, 1282: preceding L1167, 2002, 2001.
33. Suh CI, Stull ND, Li XJ, Tian W, Price MO, Grinstein S, Yaffe MB, Atkinson S, and Dinauer MC. The phosphoinositide-binding protein p40phox activates the NADPH oxidase during FcgammaIIA receptor-induced phagocytosis. *J Exp Med* 203: 1915–1925, 2006.
34. Tozawa K, al-Mehdi AB, Muzykantov V, and Fisher AB. In situ imaging of intracellular calcium with ischemia in lung subpleural microvascular endothelial cells. *Antioxid Redox Signal* 1: 145–154, 1999.
35. Vanhaesebroeck B, Leevers SJ, Ahmadi K, Timms J, Katso R, Driscoll PC, Woscholski R, Parker PJ, and Waterfield MD. Synthesis and function of 3-phosphorylated inositol lipids. *Annu Rev Biochem* 70: 535–602, 2001.
36. Vignais PV. The superoxide-generating NADPH oxidase: structural aspects and activation mechanism. *Cell Mol Life Sci* 59: 1428–1459, 2002.
37. Wei Z, Costa K, Al-Mehdi AB, Dodia C, Muzykantov V, and Fisher AB. Simulated ischemia in flow-adapted endothelial cells leads to generation of reactive oxygen species and cell signaling. *Circ Res* 85: 682–689, 1999.
38. Wei Z, Manevich Y, Al-Mehdi AB, Chatterjee S, and Fisher AB. Ca2+ flux through voltage-gated channels with flow cessation in pulmonary microvascular endothelial cells. *Microcirculation* 11: 517–526, 2004.
39. Yamamori T, Inanami O, Nagahata H, and Kuwabara M. Phosphoinositide 2-kinase regulates the phosphorylation of NADPH oxidase component p47(phox) by controlling cPKC/PKCdelta by not Akt. *Biochem Biophys Res Commun* 316: 720–730, 2004.
40. Zhang Q, Matsuzaki I, Chatterjee S, and Fisher AB. Activation of endothelial NADPH oxidase during normoxic lung ischemia is KATP channel dependent. *Am J Physiol Lung Cell Mol Physiol* 289: L954–L961, 2005.
41. Zhao G, al-Mehdi AB, and Fisher AB. Anoxia-reoxygenation versus ischemia in isolated rat lungs. *Am J Physiol* 273: L1112–L1117, 1997.
42. Zhao G, Ayene IS, and Fisher AB. Role of iron in ischemia-reperfusion oxidative injury of rat lungs. *Am J Respir Cell Mol Biol* 16: 293–299, 1997.

Address reprint requests to:
Aron B. Fisher, M.D.
Institute for Environmental Medicine
University of Pennsylvania School of Medicine
One John Morgan Building
3620 Hamilton Walk
Philadelphia, PA 19104-6068

E-mail: abf@mail.med.upenn.edu

Date of first submission to ARS Central, November 29, 2006; date of final revised submission, October 16, 2007; date of acceptance, October 16, 2007.

This article has been cited by:

1. Elizabeth R. Jacobs, Sreedhar Bodiga, Irshad Ali, Aaron M. Falck, John R. Falck, Meetha Medhora, Anuradha Dhanasekaran. 2012. Tissue protection and endothelial cell signaling by 20-HETE analogs in intact ex vivo lung slices. *Experimental Cell Research* **318**:16, 2143-2152. [CrossRef]
2. Yiqun Mo, Rong Wan, Lingfang Feng, Sufan Chien, David J. Tollerud, Qunwei Zhang. 2011. Combination effects of cigarette smoke extract and ambient ultrafine particles on endothelial cells. *Toxicology in Vitro* . [CrossRef]
3. Irshad Ali, Stephanie Gruenloh, Ying Gao, Anne Clough, John R. Falck, Meetha Medhora, Elizabeth R. Jacobs. 2011. Protection by 20-5,14-HEDGE Against Surgically Induced Ischemia Reperfusion Lung Injury in Rats. *The Annals of Thoracic Surgery* . [CrossRef]
4. Aron B. Fisher. 2011. Oxidant Stress in Pulmonary Endothelia. *Annual Review of Physiology* **74**:1, 110301101907077. [CrossRef]
5. Shampa Chatterjee , Aron B. Fisher Detection of Reactive Oxygen Species (ROS) with Altered Shear Stress in the Lung Endothelium 213-216. [Abstract] [Summary] [Full Text PDF] [Full Text PDF with Links]
6. Brian Griffith , Srikanth Pendyala , Louise Hecker , Patty J. Lee , Viswanathan Natarajan , Victor J. Thannickal . 2009. NOX Enzymes and Pulmonary Disease. *Antioxidants & Redox Signaling* **11**:10, 2505-2516. [Abstract] [Full Text HTML] [Full Text PDF] [Full Text PDF with Links]
7. Yiqun Mo, Rong Wan, Jianpu Wang, Sufan Chien, David J. Tollerud, Qunwei Zhang. 2009. Diabetes is associated with increased sensitivity of alveolar macrophages to urban particulate matter exposure. *Toxicology* **262**:2, 130-137. [CrossRef]
8. Aron B. Fisher . 2009. Redox Signaling Across Cell Membranes. *Antioxidants & Redox Signaling* **11**:6, 1349-1356. [Abstract] [Full Text PDF] [Full Text PDF with Links]
9. Yiqun Mo, Rong Wan, Sufan Chien, David J. Tollerud, Qunwei Zhang. 2009. Activation of endothelial cells after exposure to ambient ultrafine particles: The role of NADPH oxidase. *Toxicology and Applied Pharmacology* **236**:2, 183-193. [CrossRef]
10. Srikanth Pendyala , Peter V. Usatyuk , Irina A. Gorshkova , Joe G.N. Garcia , Viswanathan Natarajan . 2009. Regulation of NADPH Oxidase in Vascular Endothelium: The Role of Phospholipases, Protein Kinases, and Cytoskeletal Proteins. *Antioxidants & Redox Signaling* **11**:4, 841-860. [Abstract] [Full Text PDF] [Full Text PDF with Links]
11. Tullia Maraldi, Cecilia Prata, Diana Fiorentini, Laura Zambonin, Laura Landi, Gabriele Hakim. 2009. Induction of apoptosis in a human leukemic cell line via reactive oxygen species modulation by antioxidants. *Free Radical Biology and Medicine* **46**:2, 244-252. [CrossRef]
12. R WAN, Y MO, X ZHANG, S CHIEN, D TOLLERUD, Q ZHANG. 2008. Matrix metalloproteinase-2 and -9 are induced differently by metal nanoparticles in human monocytes: The role of oxidative stress and protein tyrosine kinase activation. *Toxicology and Applied Pharmacology* **233**:2, 276-285. [CrossRef]
13. Shampa Chatterjee, Kenneth E. Chapman, Aron B. Fisher. 2008. Lung Ischemia: A Model for Endothelial Mechanotransduction. *Cell Biochemistry and Biophysics* **52**:3, 125-138. [CrossRef]
14. Dipak K. Das Methods in Redox Signaling . [Citation] [Full Text HTML] [Full Text PDF] [Full Text PDF with Links]